

Deductive geoacoustic inversion: Robustness to water depth mismatch

M. A. Ainslie, R. A. Laker

CORDA Ltd, Apex Tower, 7 High Street, New Malden, Surrey, KT3 4LH, UK.
michael.ainslie@corda.co.uk, robert.laker@corda.co.uk

Abstract

A geoacoustic inversion model is described. A fluid sea bed model is assumed, with geoacoustic properties described by a total of nine parameters. A further five geometric parameters, including water depth, are also included in the search. The sound speed profile in the water is assumed known. Synthetic data in the range 50-500 Hz are used to test the model in range-independent environments. Robustness is considered by introducing mismatches in the water depth and other environmental parameters.

1. Introduction

The objectives of this paper are to describe a geoacoustic inversion model and to demonstrate its robustness to environmental mismatch in general and to water depth mismatch in particular. Of interest are the effects of:

- unknown water depth or bathymetry;
- unknown sediment layering;
- sea bed rigidity.

A synthetic data set that includes test cases covering each of these effects was produced for the Vancouver 97 workshop [1]. The relevant test cases are WA (unknown water depth), N (unknown layering) and EL (elastic sea bed). DREAM results for cases N and EL are presented in reference [2]. Here we concentrate on case N (unknown sediment layering), to which we add a water depth mismatch by deliberately introducing an error in this parameter of up to 2 m.

2. Inversion Method

2.1 The DREAM Model

The basic inversion algorithm used by DREAM (Deductive Rapid Environmental Assessment Model) is described in reference [2]. The sea bed is described by the 9-parameter model shown in Figure 1. DREAM searches for these 9 parameters and 5 more describing the geometry: source range r_s and depth z_s ; array tilt ϕ_a and depth z_a ; and water depth H .

The DREAM algorithm involves successive iterations over three phases at high, medium and low frequency (Figure 2). Phases 1 and 2 are exhaustive searches in two dimensions at a time. Phase 3 is a six-dimensional search using a global optimisation algorithm known as differential evolution (DE). The version of DREAM used here (v3.3) differs from [2] as follows:

- the high frequency exhaustive search (phase 1) is over sound speed and *water depth* (instead of sound speed and density);
- the density inversion, previously in phase 1, now appears in the low frequency DE search (phase 3);
- new (exhaustive) searches are introduced for array depth and tilt angle in phase 1 and 2 (not shown).

In addition, two different search strategies (see Section 2.2) are available, designed for known and unknown source position.

The justification for delaying the sediment density to phase 3 is that an accurate value of density is not required to obtain an accurate sound speed in phase 1 [3]. It is sufficient to estimate the density ρ_{sed} through its correlation with the sediment sound speed c_0 , and for this purpose we use the Hamilton-Bachman formula for continental terrace sediments [4] in the form

$$\rho_{sed}(c_0) = 1.289 + 0.0453\sqrt{c_0(\text{m/s}) - 1520.45} \quad \text{g/cm}^3 \quad (1)$$

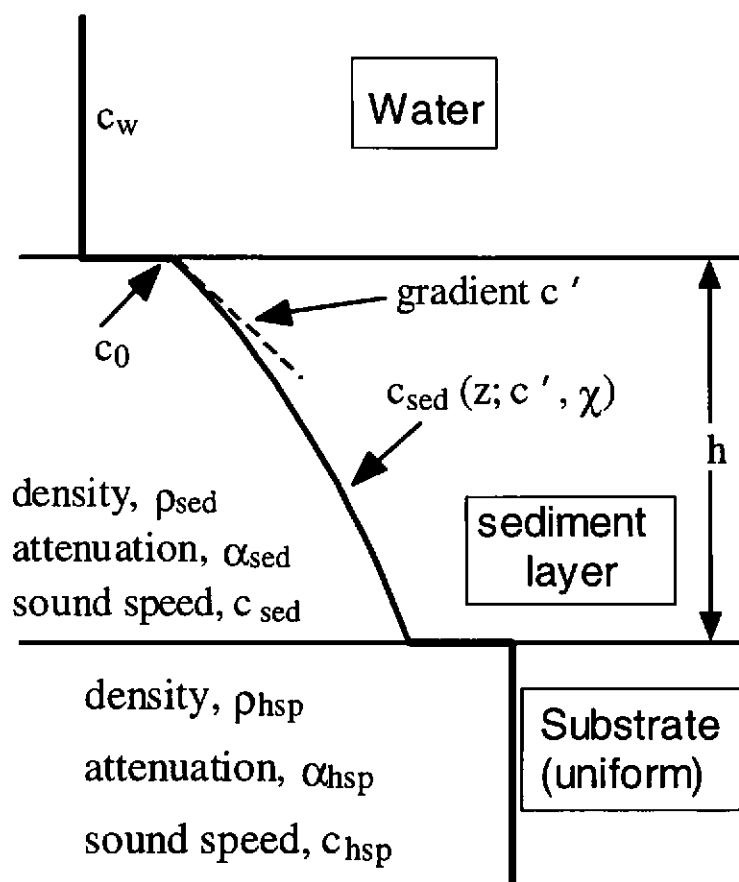


Figure 1. Nine parameter sea bed model ($c_0, c', \chi, h, \rho_{sed}, \alpha_{sed}, c_{hsp}, \rho_{hsp}, \alpha_{hsp}$). The parameter χ determines the sound speed curvature [2].

2.2 Search Strategies

2.2.1 Known source position: Two-pass strategy

If the geometry (primarily the source position and array depth) is known accurately we adopt a "two-pass" strategy, by which we mean that two full iterations of Figure 2 are carried out. The source position and array geometry is either frozen or allowed to vary within some small tolerance.

2.2.2 Unknown source position: Four-pass strategy

For an unknown source position a total of four passes through Figure 2 are carried out. The first two are used to determine the source-receiver geometry (r_s, z_s, ϕ_a, z_a) using a coarse environment grid. Pass 3 refines the r_s and ϕ_a estimates with z_s and z_a fixed, and at the same time performs the bulk of the geoacoustic inversion. The final pass refines the geoacoustic parameters with the geometric parameters frozen (except water depth).

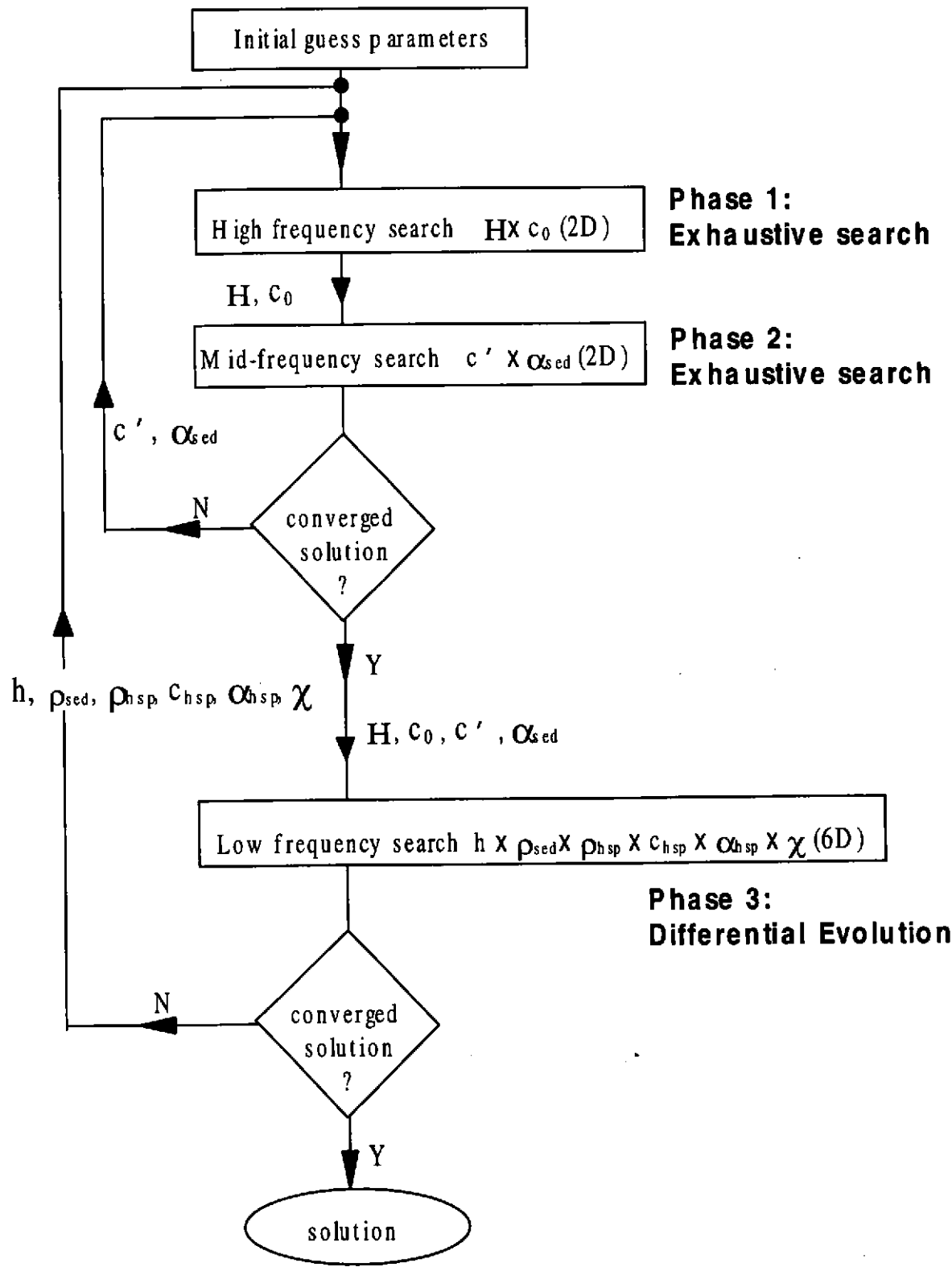


Figure 2. Flow diagram of the three-frequency deductive search model (DREAM). In general, phases 1 and 2 also include an exhaustive search for parameters determining the source geometry (r_s, z_s) and receiver geometry (ϕ_r, z_r).

2.3 Effect of Water Depth Mismatch

It is shown in reference [5] that a strong correlation exists (in expected inversion results) between the water depth and other geometric parameters. The reason for this correlation is that the pressure field for a water depth H due to a source at (r_s, z_s) can be simulated to a close approximation in water depth H' by an image source at (r_s', z_s') where [5]

$$r_s' = r_s (H'/H)^2 \quad (2a)$$

and

$$z_s' = z_s H'/H \quad (2b)$$

It follows that, for a search in which all three parameters are allowed to vary, a family of solutions $\{r_s', z_s', H'\}$ satisfying (2) may be found, all with a similar fitness to the true solution $\{r_s, z_s, H\}$. If we choose to fix one of the three parameters (say water depth), the other two follow from (2). In other words, for a fixed water depth H' and true water depth H , the source will be uniquely localised at the image position (r_s', z_s') instead of the true position (r_s, z_s) . There is therefore a localisation error given by

$$\Delta r_s = r_s' - r_s = 2(H' - H)r_s/H \quad (3a)$$

$$\Delta z_s = z_s' - z_s = (H' - H)z_s/H. \quad (3b)$$

The above equations assume a range independent environment (with uniform water depth H). They are quoted in a more general form for a range-dependent bathymetry in the Appendix.

For a geoacoustic inversion we are interested not in the source position but in the geoacoustic parameters themselves. How are these affected by the localisation error? This question is addressed in Section 3 by carrying out a sequence of inversions, each with a different fixed value for the water depth within $\pm 2\%$ of the true value.

3. Results

We now consider case Na from Vancouver 97 [1]. This case comprises multiple uniform sub-layers making up a total sediment thickness of 55 m. For details see reference [2] which includes a comparison of DREAM v3.2 results with inversions by Siderius *et al.* [6] and Fallat and Dosso [7]. The multiple sediment layering means that there is inevitably a mismatch in the sediment profile. Here we deliberately introduce a mismatch in water depth as well. Table 1 shows inversion results for assumed water depths between 98 m and 102 m, using a vertical line array at a range of 5 km and frequencies 50, 100 and 500 Hz. The geometry is fixed at known values except for the source range, which is allowed to vary between 4.8 and 5.2 km. It is apparent from Table 1 that the main effect of a water depth mismatch of up to ± 2 m is to shift the source position in range, while the sea bed parameters are basically unchanged. The size of the observed range shift Δr_s is in reasonable agreement with that predicted by (3a). The inverted sound speed (c_0) and gradient (c') never differ by more than 11 m/s and 2.1 /s from their values for the correct water depth. This robustness to a water depth mismatch of up to 2% is exploited in a companion paper presenting inversion results for an acoustic trial in the Strait of Sicily [8].

Strictly speaking the source and receiver depths should be displaced from their true positions as described in the Appendix. These depth shifts are small compared with the range shift and for simplicity are neglected here. An improvement in the inversion results may be possible if the depth shifts are allowed for.

4. Conclusions

Our main conclusion is that a small error (up to 2%) in assumed water depth does not appear to alter the result of geoacoustic inversion in shallow water, although it does result in a significant shift in the apparent source position by up to 4% in range. The largest discrepancy in sound speed (compared with its value for the correct water depth) is 11 m/s.

This is important because, provided the source position is treated as an unknown parameter, there is no need to devote any computational effort to identifying a precise value for the water depth.

Assumed water depth H' (m)	Fitness ^(b)	Δr_s (m)	h_{sed} (m)	c_0 (m/s)	c' (/s)	ρ_{sed} (g/cm ³)	α_{sed} (dB/ λ)
98.0	0.95	-200	46.5	1500	8.3	1.58	0.17
99.0	0.97	-100	41.6	1502	7.0	1.51	0.21
99.5	0.99	-64	47.8	1510	7.3	1.47	0.22
100.0	0.99	-12	53.4	1511	6.2	1.47	0.22
100.5	0.99	+16	45.1	1522	5.3	1.44	0.25
101.0	0.98	+72	45.5	1522	5.8	1.44	0.22
101.5	0.96	+120	45.8	1521	6.9	1.25	0.29
102.0	0.92	+184	37.6	1514	8.1	1.25	0.32
100.0 ^(a)	0.998	(0)	61.0	1505	7.4	1.47	0.24

(a) Reference solution for known geometry using DREAM v3.2 [2].

(b) Bartlett processor power (correlation squared), averaged incoherently over frequency.

Table 1. Inversion results (average of fittest half of final DE population).

5. Appendix – Effect of Range-dependent Bathymetry

The purpose of this Appendix is to describe the effect on (2) and (3) of variations in the true water depth $H(r)$ along the propagation path between source and receiver. Harrison and Siderius [5] show that the field (as determined by the relative phase delay between successive multipaths) is determined to a good approximation by the parameters $z_s/H(r_s)$, $z_r/H(0)$ and $\int_0^{r_s} dr/H^2(r)$, provided that bathymetry variations are gradual. It follows that, for an assumed uniform water depth H' , the image source position required to reproduce the field is given by

$$r'_s = r_s (H'/H_e)^2 \tag{4a}$$

and

$$z'_s = z_s H'/H(r_s) \tag{4b}$$

where H_e is an effective uniform water depth defined by [5]

$$H_e^2 = \frac{r_s}{\int_0^{r_s} dr/H(r)^2} \tag{5}$$

The error in source position (the distance from true to image source) is therefore given by

$$r'_s - r_s = r_s [(H'/H_e)^2 - 1] \tag{6a}$$

and

$$z'_s - z_s = z_s [H'/H(r_s) - 1] \tag{6b}$$

The receiver depth scales in the same way so that

$$z'_r - z_r = z_r [H'H(0) - 1] \quad (6c)$$

If the bathymetry variations are small, (6a) can be further approximated by

$$r'_s = r_s \approx 2r_s (H' - H_e)/H_e \quad (7)$$

References

- [1] Tolstoy A, Chapman NR and Brooke G. Workshop '97: Benchmarking for geoacoustic inversion in shallow water, in reference [9], 1-28.
- [2] Ainslie MA, Hamson RM, Horsley GD, James AR, Laker RA, Lee MA, Miles DA and Richards SD. Deductive multi-tone inversion of seabed parameters. *J. Comp. Acoust.* 2000; 8(2): 271-284.
- [3] Hamson RM and Ainslie MA. Broadband geoacoustic deduction, in [9], March & June 1998, pp 45-60.
- [4] Hamilton EL and Bachman RT. Sound velocity and related properties of marine sediments. *J. Acoust. Soc. Am.* 1982; 72: 1891 - 1904.
- [5] Harrison CH and Siderius M. Correlations between search parameters in geoacoustic inversion, in *Proc. Fifth European Conference on Underwater Acoustics* (eds Chevret P and Zakharia ME). Lyon, France, 2000.
- [6] Siderius M, Gerstoft P and Nielsen P. Broadband geo-acoustic inversion from sparse data using genetic algorithms, in reference [9], 117-134.
- [7] Fallat MR and Dosso SE. Geoacoustic inversion via local, global and hybrid algorithms. *J. Acoust. Soc. Am.* 1999; 105: 3219-3230.
- [8] Ainslie MA, Laker RA and Hamson RM. Deductive geoacoustic inversion: Application to measured data in the Strait of Sicily, in 'Acoustical Oceanography', *Proceedings of the Institute of Acoustics Vol. 23 Part 2, 2001*, T G Leighton, G J Heald, H Griffiths and G Griffiths, (eds.), Institute of Acoustics, (this volume), pp. 66-73.
- [9] Chapman R and Tolstoy A (eds). Benchmarking geoacoustic inversion methods. Special Issue, *J. Comp. Acoust.* 6 (1&2), March & June 1998.